MCB
Journals.ASM.org

Mot1 Redistributes TBP from TATA-Containing to TATA-Less Promoters

Gabriel E. Zentner,[a] Steven Henikoff[a,b]

Basic Sciences Division[a] and Howard Hughes Medical Institute,[b] Fred Hutchinson Cancer Research Center, Seattle, Washington, USA

The Swi2/Snf2 family ATPase Mot1 displaces TATA-binding protein (TBP) from DNA *in vitro*, but the global relationship between Mot1 and TBP *in vivo* is unclear. In particular, how Mot1 activates transcription is poorly understood. To address these issues, we mapped the distribution of Mot1 and TBP on native chromatin at base pair resolution. Mot1 and TBP binding sites coincide throughout the genome, and depletion of TBP results in a global decrease in Mot1 binding. We find evidence that Mot1 approaches TBP from the upstream direction, consistent with its *in vitro* mode of action. Strikingly, inactivation of Mot1 leads to both increases and decreases in TBP-genome association. Sites of TBP gain tend to contain robust TATA boxes, while sites of TBP loss contain poly(dA-dT) tracts that may contribute to nucleosome exclusion. Sites of TBP gain are associated with increased gene expression, while decreased TBP binding is associated with reduced gene expression. We propose that the action of Mot1 is required to clear TBP from intrinsically preferred (TATA-containing) binding sites, ensuring sufficient soluble TBP to bind intrinsically disfavored (TATA-less) sites.

TATA-binding protein (TBP) is a general regulator of eukaryotic transcription required for initiation by all three eukaryotic RNA polymerases (1). TBP lies at the center of a complex transcriptional network (2) and as such is regulated by a diverse array of factors. One such TBP-regulating protein is modifier of transcription 1 (Mot1), a highly conserved (3) and essential (4, 5) member of the Swi2/Snf2 ATPase family. Mot1 uses the energy derived from ATP hydrolysis to remove TBP from DNA (6), and the mechanism of action of Mot1 is perhaps the best understood of all Swi2/Snf2-like ATPases. Mot1 recognizes TBP from upstream, associating with TBP from above via its acidic loops. The Swi2/Snf2 ATPase domain of Mot1 contacts DNA ~17 bp upstream of TBP and translocates toward TBP, loosening its association of TBP with DNA. Last, the latch of Mot1 occupies the DNA-binding groove of TBP, displacing the Mot1-TBP complex from DNA and preventing TBP from rebinding DNA (7–10).

The finding that Mot1 displaces TBP from DNA (6) led to the hypothesis that it would act primarily as a transcriptional repressor. However, numerous transcriptional profiling studies have established that loss of Mot1 both increases and decreases gene expression (4, 5, 11–18). Furthermore, loss of Mot1 has also been found to reduce TBP association with some promoters (11, 12, 18–21). Several models have been put forward to reconcile these findings with the well-characterized TBP-displacing activity of Mot1: (i) a preinitiation complex (PIC) remodeling model, wherein Mot1 alters the PIC conformation, presumably via interaction with TBP followed by ATP hydrolysis and translocation, to enhance transcriptional permissiveness (13); (ii) a PIC formation model, wherein the TBP-Mot1 complex nucleates an alternative, transcriptionally competent PIC (22); (iii) a nucleosome remodeling model, wherein Mot1 participates directly or indirectly in nucleosome remodeling, facilitating binding of TBP by excluding nucleosomes from promoters (23); (iv) a recruitment model, wherein Mot1 actively recruits TBP to chromatin (11); and (v) a redistribution model, where loss of Mot1 function leads to transfer of TBP from intrinsically unfavorable to favorable binding sites, as there is insufficient Mot1 action to clear TBP from its favored sites (18, 22). Reconciling the positive effects of Mot1 on a subset of genes with its known *in vitro* activity remains an important unsolved problem in the field.

To address this problem, we set out to elucidate the relationship between Mot1 and TBP across the genome. We first mapped the distribution of Mot1 and TBP on native chromatin at base pair resolution. Consistent with *in vitro* studies of Mot1 function, our results indicate that Mot1 approaches TBP from upstream *in vivo*. Nuclear depletion of TBP resulted in attenuation of Mot1-genome association, consistent with a role for TBP in Mot1 recruitment to chromatin. Surprisingly, while Mot1 inactivation led to a modest increase in TBP binding when all promoters were considered, the most robust sites of TBP binding were more likely to lose TBP than to gain TBP upon Mot1 inactivation. Sites of TBP gain contained strong TATA sequences, while those that lost TBP contained poly(dA-dT) tracts that could contribute to nucleosome exclusion. Genes that gained TBP at their promoters tended to show increased expression upon Mot1 inactivation, while those that lost TBP were more likely to show decreased expression. We suggest that the primary role of Mot1 *in vivo* is to clear TBP from intrinsically preferred (TATA-containing) promoters to ensure sufficient soluble TBP to bind intrinsically disfavored (TATA-less) sites and that the positive effect of Mot1 on transcription can be attributed to its maintenance of a balance of TBP levels between TATA-containing and TATA-less promoters.

Received 12 September 2013 **Accepted** 11 October 2013
Published ahead of print 21 October 2013
Address correspondence to Steven Henikoff, steveh@fhcrc.org.
Supplemental material for this article may be found at http://dx.doi.org/10.1128/MCB.01218-13.

doi:10.1128/MCB.01218-13
The authors have paid a fee to allow immediate free access to this article.

TABLE 1 Yeast strains used in this study

Strain	Background	Genotype	Source
GZY8	W1588-4C	*MAT***a** *ade2-1 can1-100 his3-11,15 leu2-3,112 trp1-1 ura3-1 RAD5*$^+$ *MOT1-3FLAG-kanMX4*	This study
GZY51	W303	*MAT*α *ade2-1 can1-100 his3-11,15 leu2-3,112 trp1-1 ura3-1 tor1-1 fpr1*::*natMX4 RPL13A-2*×*FKBP12*::*TRP1 TBP-FRB-kanMX6 MOT1-3FLAG-hphMX4*	This study
HHY154	W303	*MAT*α *ade2-1 can1-100 his3-11,15 leu2-3,112 trp1-1 ura3-1 tor1-1 fpr1*::*natMX4 RPL13A-2*×*FKBP12*::*TRP1 TBP-FRB-kanMX6*	EUROSCARF
HHY168	W303	*MAT*α *ade2-1 can1-100 his3-11,15 leu2-3,112 trp1-1 ura3-1 tor1-1 fpr1*::*natMX4 RPL13A-2*×*FKBP12*::*TRP1*	EUROSCARF
YAD155	YPH499	*MAT***a** *ura3-52 lys3-52 lys2-801*^{a} *ade2-101*^{o} *trp1*Δ*63 his3*Δ*200 leu2*Δ*1 mot1*::*TRP1* pAV20 (*EE-MOT1*$^+$ *LEU2*$^+$ *CEN ARS*) *TBP-13MYC-HIS3MX6*	David Auble
YAD156	YPH499	*MAT***a** *ura3-52 lys3-52 lys2-801*^{a} *ade2-101*^{o} *trp1*Δ*63 his3*Δ*200 leu2*Δ*1 mot1*::*TRP1* pMot221 (*mot1-42 LEU2*$^+$ *CEN ARS*) *TBP-13MYC-HIS3MX6*	David Auble

MATERIALS AND METHODS

***Saccharomyces cerevisiae* methods.** *Saccharomyces cerevisiae* (yeast) cells were grown at 30°C in yeast extract-peptone-dextrose (YPD) medium. The TBP-AA/Mot1-3FLAG (AA stands for anchor-away) strain was constructed by PCR-based tagging of Mot1 in strain HHY154 (24) using p3FLAG-hyg, a derivative of p3FLAG-kanMX (25). Cells were treated with 1 μg/ml rapamycin (Sigma) for 1 h to induce nuclear depletion of TBP. For spot assays, cells grown overnight were diluted to an optical density at 600 nm (OD_{600}) of 1.0, 3-μl portions of five 10-fold serial dilutions were plated on YPD with and without 1 μg/ml rapamycin, and the plates were photographed after ~36 h of growth at 30°C. Mot1 was inactivated by incubation of the *mot1-42* strain at 35°C for 45 min. Nuclear isolation, micrococcal nuclease (MNase) digestion, and chromatin preparation were performed as described previously (26). Yeast strains used in this study are listed in Table 1.

ORGANIC profiling. ORGANIC-seq (sequencing of occupied regions of genomes from affinity-purified naturally isolated chromatin [ORGANIC]) was performed as described previously (26). For TBP-13MYC ORGANIC experiments, 12 μg of mouse anti-Myc (9E10 [sc-40x; Santa Cruz]) was bound to 100 μl protein G DynaBeads (Invitrogen) that had been prewashed three times with 1 ml of phosphate-buffered saline containing 0.5% bovine serum albumin (PBS–0.5% BSA) at 4°C for at least 4 h. Antibody-coupled beads were washed three times with 1 ml PBS–0.5% BSA prior to use.

Sequencing libraries were prepared using our previously described modification of the standard Illumina protocol (27), except that TruSeq adapters were used for multiplexing and the ratio of sample to Ampure beads was changed from 5:9 to 1:1 in the two cleanup steps to compensate for the longer length of the TruSeq adapters. Libraries were sequenced for 25 cycles in paired-end mode on the Illumina HiSeq 2000 platform at the Fred Hutchinson Cancer Research Center (FHCRC) Genomics Shared Resource.

Data analysis. Sequenced fragments were processed, aligned, and analyzed as described previously (26). Signal tracks were visualized with SignalMap (Nimblegen). A list of yeast transcription start sites (TSSs) was obtained from the *Saccharomyces* Genome Database (SGD) (http://www.yeastgenome.org/) for analysis of the ends using previously published Perl scripts (28) as described previously (26). TBP ChIP-exo (chromatin immunoprecipiation followed by λ exonuclease digestion and sequencing) data and TATA box annotations were obtained from Rhee and Pugh (29). Peaks were called using a threshold determined by taking the average of normalized counts across the genome and adding an empirically determined multiple of the standard deviation of genome-wide normalized counts. Base positions above the threshold were grouped into a discrete peak if they were within 10 bp of one another. The midpoint of a peak was taken to be the position of the base with the highest normalized count value of all bases within the peak. A 56-bp window around each peak midpoint was used for overlap analysis and motif discovery. See Data Set S1 in the supplemental material for a list of TBP peaks and their occupancies. Peak occupancies from the TBP-AA/Mot1 ORGANIC and *mot1-42*/TBP ORGANIC experiments are given in Data Sets S2 and S3, respectively, in the supplemental material. Occupancies were $\log_{10}$ transformed for correlation analysis and two-dimensional histogram generation. For chi-square analysis, the numbers of RNA polymerase II (Pol II) (6,744, the sum of mRNA and transposon genes) and Pol III (279 [30]) genes were used to calculate the expected frequencies of Pol II and Pol III genes in each peak set. For the 10-min MNase time point (266 peaks), 255 Pol II genes and 11 Pol III genes were expected. For the 2.5-min MNase time point (258 peaks), 248 Pol II genes and 10 Pol III genes were expected. MEME-ChIP (31) was used to search peaks for motifs. TBP peaks with matches to the DREME TATAWAWR position-specific scoring matrix (PSSM) at a *P*-value threshold of <0.0001 were determined with FIMO (32).

Sequencing data accession number. Sequencing data have been deposited with GEO (GSE44200).

RESULTS

Global mapping of Mot1 and TBP on native chromatin. To study the genomic binding of Mot1 and its relationship to TBP, we applied the ORGANIC (occupied regions of genomes from affinity-purified naturally isolated chromatin) profiling method that we had previously used to profile other SWI/SNF family chromatin regulators (26) and transcription factors (S. Kasinathan, G. A. Orsi, G. E. Zentner, K. Ahmad, and S. Henikoff, submitted for publication). Un-cross-linked chromatin from yeast strains harboring epitope-tagged Mot1 or TBP alleles was digested for 2.5 min or 10 min with micrococcal nuclease (MNase), immunoprecipitated using antibodies directed against the appropriate epitope, and Mot1/TBP-associated and input DNA samples were prepared for sequencing using a modified library preparation protocol that allows recovery of fragments as short as ~25 bp (27), enabling the generation of base pair resolution maps of Mot1 and TBP binding to the yeast genome. The majority of reads for input samples were of approximately nucleosomal size, with maxima between 150 and 170 bp (Fig. 1A). Mot1 and TBP immunoprecipitation (IP) samples displayed notable enrichment of subnucleosome-size fragments (Fig. 1A), suggesting that Mot1 and TBP participate in the protection of extended stretches of naked DNA, likely within promoters in conjunction with preinitiation complexes (PICs), while nucleosome-size particles were depleted from Mot1 and TBP IPs. We also compared TBP ORGANIC signal to ChIP-exo (chromatin immunoprecipiation followed by λ exonuclease digestion and sequencing) signal (29) at TATA boxes. This analysis revealed a notable correlation between results obtained by the two methods (2.5-min MNase $R^2 = 0.57$; 10-min MNase $R^2 = 0.63$). We detected robust binding of Mot1 and TBP in intergenic regions throughout the genome (Fig. 1B). Mot1 and

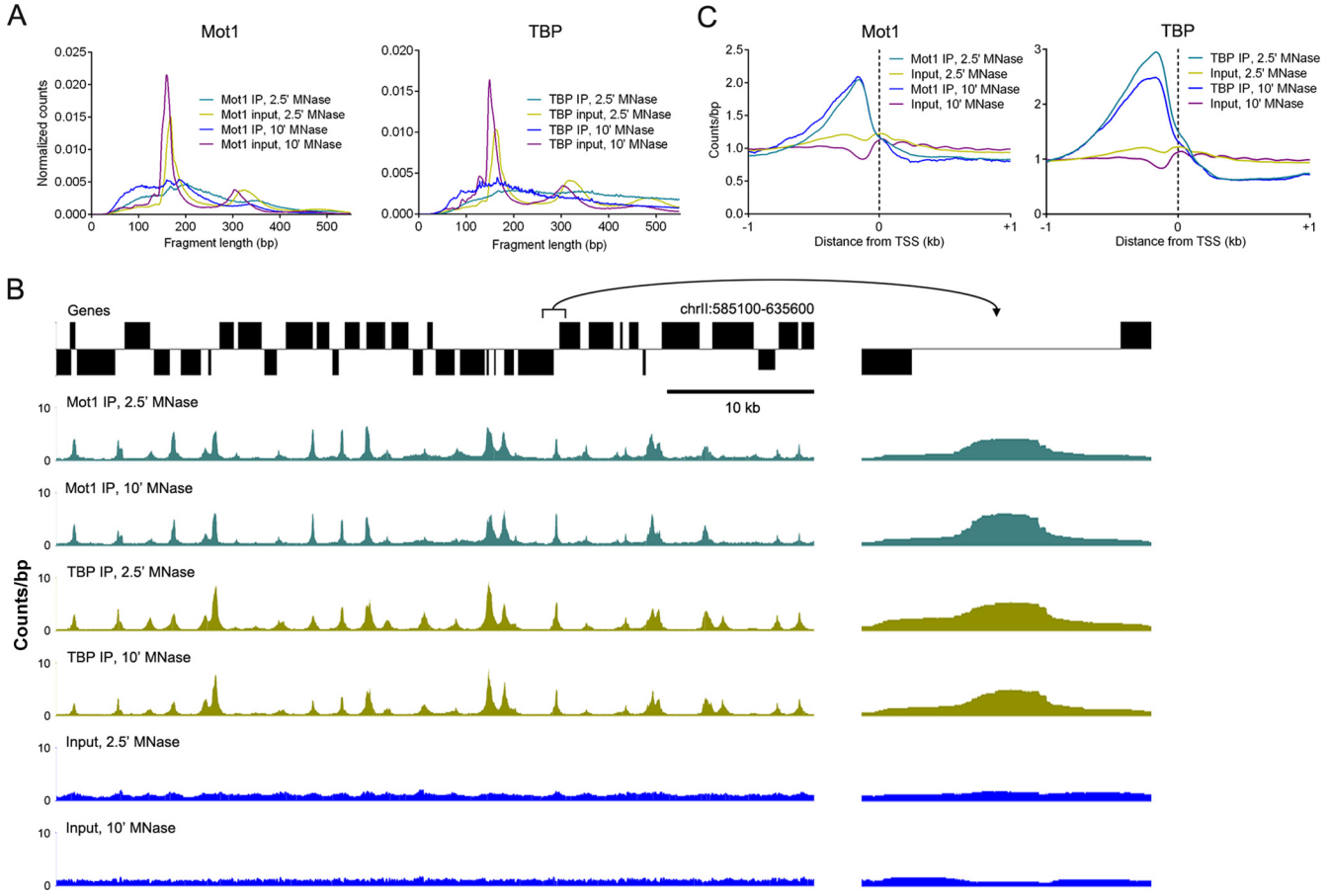

FIG 1 Genome-wide mapping of Mot1 and TBP on native chromatin. (A) Length distributions of paired-end fragments from Mot1 and TBP IP and input samples. Distributions were normalized such that the sum of all counts was equal to 1. (B) Tracks of TBP and Mot1 2.5-min (2.5′) and 10-min (10′) MNase IP and input data along a representative portion of the yeast genome. A zoomed-in view of a single region of Mot1 and TBP enrichment is shown to the right of the tracks. chrII, chromosome II. (C) Aggregate plots of 2.5′ and 10′ MNase Mot1, TBP, and input counts/bp at all TSSs.

TBP enrichment was particularly strong just upstream of transcription start sites (Fig. 1C), consistent with the known functions of these proteins at promoters.

Mot1 and TBP cooccupy sites across the genome. To facilitate further analysis of the relationship between Mot1 and TBP binding, we called peaks on our TBP ORGANIC data sets using a thresholding approach. For the 2.5-min MNase time point, this yielded 3,272 peaks, and for the 10-min MNase time point, it gave 3,002 peaks (see Data Set S1 in the supplemental material). Peaks were highly reproducible across the 4-fold range of MNase digestion: all 3,002 peaks in the 10-min MNase sample overlapped peaks in the 2.5-min MNase sample (Fig. 2A). We then determined the occupancy of each peak by determining the area under the curve (that is, the total number of counts comprising the peak) for a 200-bp window centered on each peak midpoint and found that their occupancies were highly correlated ($R^2 = 0.91$) (Fig. 2B). We also detected notable enrichment of Mot1 around TBP peaks (Fig. 2C).

Previous cross-linked chromatin immunoprecipitation with microarray technology (X-ChIP-chip) and cross-linked chromatin immunoprecipitation-DNA sequencing (X-ChIP-seq) studies have demonstrated that Mot1 and TBP bind highly similar sets of sites throughout the genome (12, 33–35). Furthermore, it has been suggested that, at some promoters, there are fixed ratios of Mot1 to TBP (36). Our observations of close correspondence between Mot1 and TBP peaks (Figs. 1B and 2C) are consistent with the idea of a relationship between Mot1 and TBP binding. To test this on a genome-wide scale, we compared the occupancy of Mot1 and TBP at TBP peaks and detected essentially no correlation between TBP and Mot1 enrichment when all 10-min MNase peaks were considered together ($R^2 = 0.009$) (Fig. 2D). However, it was clear from the scatterplot that in terms of the ratio of Mot1-to-TBP enrichment, there are multiple classes of TBP peaks. Most conspicuous was a distinct cluster of sites with very high TBP occupancy but relatively low Mot1 occupancy. To determine the nature of these sites, we analyzed the genes associated with TBP peaks displaying a Mot1/TBP ratio of <0.1 and $\log_{10}$ TBP enrichment of >3.5. Of the 266 10-min MNase peaks meeting these criteria, 1 (0.38%) was associated with a Pol III-transcribed snRNA (snR6) and 181 (68.0%) were associated with tRNA genes (see Data Set S1 in the supplemental material). The remainder of these sites were associated with protein-coding genes (71 [26.7%]), retrotransposons (11 [4.1%]), the 5′ external transcribed spacer (ETS) of ribosomal DNA (rDNA) (1 [0.38%]), and a single Pol II-transcribed snRNA (snR33 [0.38%]). Similar results were obtained with the 2.5-min MNase peak set (Pol III

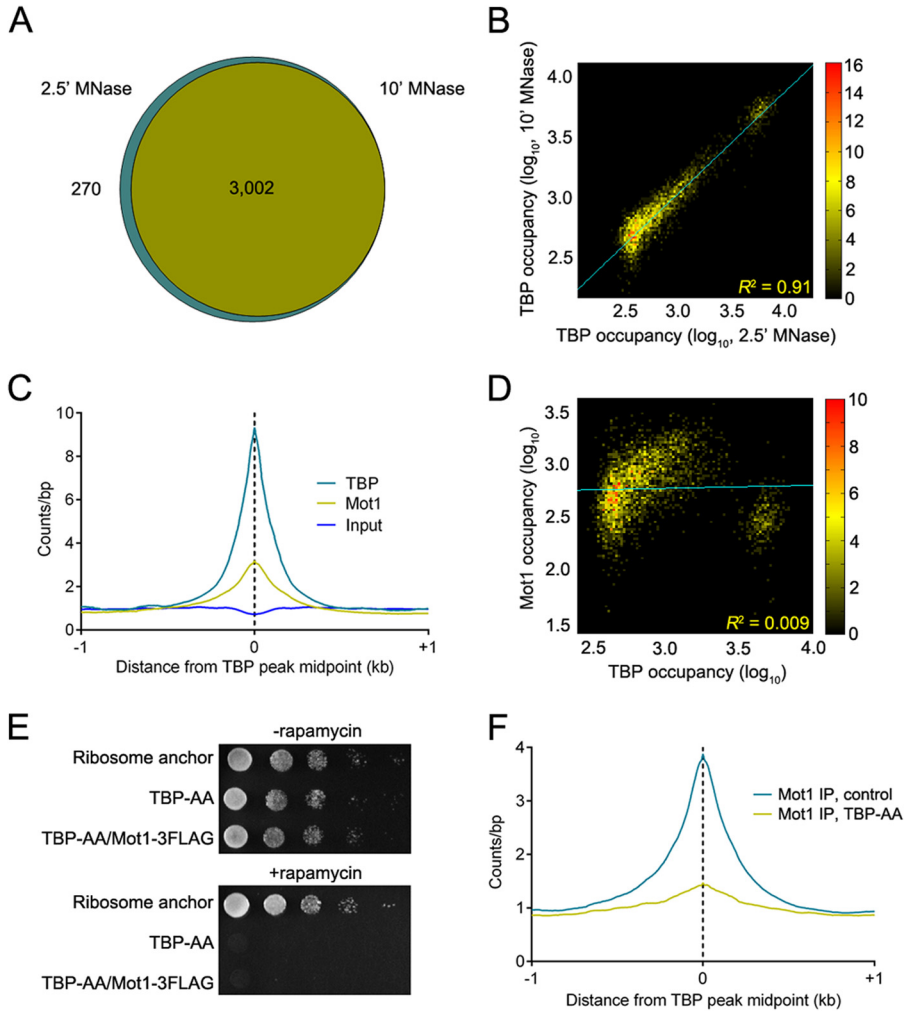

FIG 2 TBP and Mot1 cooccupy thousands of sites, and Mot1 depends on TBP for genomic association. (A) Venn diagram showing overlap of TBP ORGANIC peaks called from the 2.5 min (2.5′) and 10′ MNase data sets. (B) Two-dimensional histogram comparing enrichment of TBP at the 3,002 overlapping TBP peaks after 2.5 min (2.5′) and 10 min (10′) MNase digestion. Sites of high TBP enrichment, found in the top right corner of the histogram, are mainly tRNA promoters. The blue line represents a regression line. (C) Aggregate plot of TBP and Mot1 IP data and input data (10′ MNase) around 3,002 TBP peaks called on the 10′ MNase data set. (D) Two-dimensional histogram comparing Mot1 and TBP occupancy levels at TBP peaks. (E) Spot assay to characterize the TBP-AA/Mot1-3FLAG strain, demonstrating that epitope tagging of Mot1 does not interfere with the previously reported lethality of TBP-AA (24). (F) Aggregate plot of Mot1 IP data (10′ MNase) around 3,002 TBP peaks with or without AA-mediated depletion of TBP.

snRNAs [snR6, RPR1], 2/258 [0.75%]; tRNAs, 170/258 [65.9%]; protein-coding genes, 83/258 [32.3%]; retrotransposons, 4/258 [1.6%]). In both cases, this cluster of peaks was dominated by TBP binding sites associated with Pol III promoters ($P < 10^{-300}$ for both MNase time points by chi-square analysis). These observations are consistent with previous studies showing that Pol III promoters tend to be very highly enriched for TBP relative to Mot1 (36, 37).

Mot1 requires TBP for chromatin binding. As previous studies have shown that, at a few promoters, loss of TBP reduces Mot1 binding (36), we set out to determine the global effects of TBP loss on Mot1-genome association. To this end, we employed the anchor-away (AA) method, which has been successfully used to deplete a number of nuclear proteins including TBP (24). We epitope tagged Mot1 in the TBP-AA background and confirmed that the presence of tagged Mot1 did not interfere with the previously reported lethality of TBP nuclear depletion (Fig. 2E). We then performed Mot1 ORGANIC profiling following rapamycin treatment to deplete TBP and compared the enrichment of Mot1 at TBP peaks with and without TBP depletion. We observed a global reduction in Mot1 binding at TBP peaks relative to the genome as a whole (Fig. 2F; see Data Set S2 in the supplemental material), consistent with a role for TBP in recruiting Mot1 to chromatin.

Mot1 associates with chromatin upstream of TBP. *In vitro*, Mot1 associates with an ~17-bp DNA "handle" upstream of TBP and recognizes TBP from upstream prior to TBP removal (7, 9, 10). While binding of Mot1 to DNA upstream of TBP is essential for TBP displacement *in vitro*, it has been unclear whether this directional engagement of Mot1 occurs *in vivo* due to the limited resolution of widely used X-ChIP methods (38). We thus set out to determine whether there is directionality in the recognition of TBP by Mot1 *in vivo*. To allow for proper orientation of TBP peaks, which contain no intrinsic strand information, we used

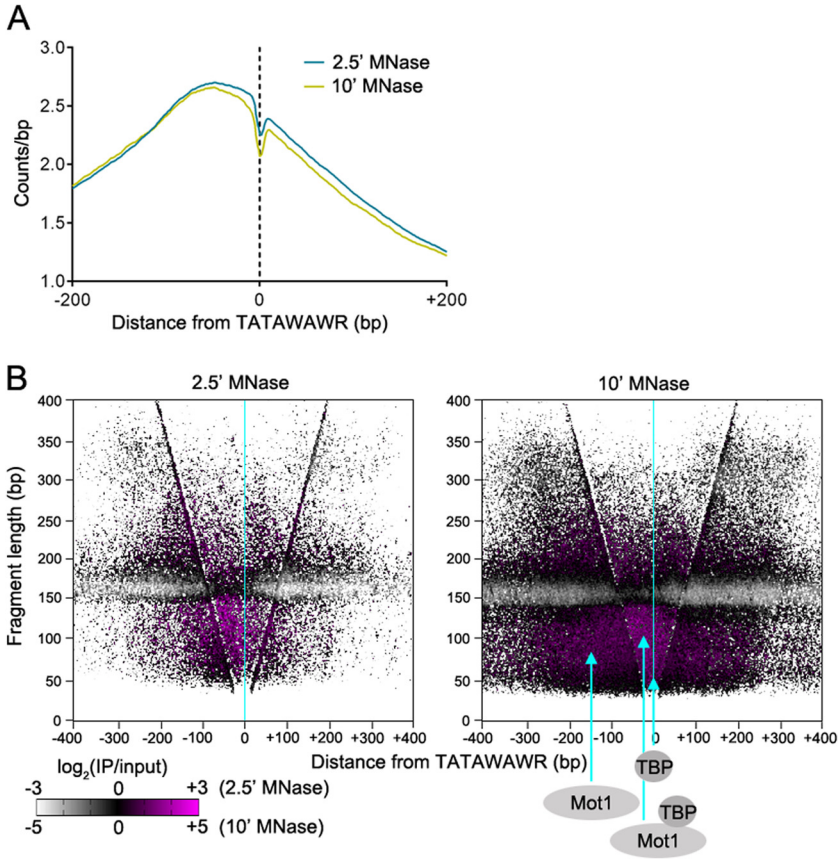

FIG 3 Mot1 binds DNA upstream of TBP. (A) Aggregate plot of 2.5′ and 10′ MNase Mot1 ORGANIC signal at 438 TBP peaks containing a strong match to the TATAWAWR TATA box consensus sequence. (B) V-plots of 2.5′ and 10′ MNase $\log_2$ (Mot1 IP/input) signal at the 438 TBP peaks analyzed in panel A. The cyan line through each plot denotes the TATAWAWR midpoint. Particles presumed to give rise to the observed fragments are depicted schematically below the right panel. A lack of interaction between Mot1 and nucleosomes is demonstrated by the white/gray particles observed upstream and downstream of TATAWAWR at 150 to 160 bp.

FIMO (32) to search our TBP peak set for strong ($P < 0.0001$) matches to the TATAWAWR consensus sequence (29). This generated a list of 438 TBP peaks with motif coordinates and strand information. Plotting of the aggregate Mot1 signal around these sites revealed that it was enriched directly upstream of the TATA WAWR motif and, by extension, TBP (Fig. 3A). We also noted a slight enrichment of Mot1 downstream of the TATAWAWR motif (Fig. 3A). As TBP sometimes binds to promoters in the wrong orientation to support productive PIC formation (39), this upstream enrichment may represent Mot1 recognizing "backwards" TBP from the opposite orientation.

We also used V-plotting (27) to assess the spatial relationship of Mot1 and TBP at promoters containing the TATAWAWR motif. In this approach, the midpoint of each paired-end fragment is assigned a dot, which is then plotted in two-dimensional space. Its *x* coordinate represents the distance of the fragment midpoint from a defined genomic feature, while its *y* coordinate represents the length of the corresponding fragment. We generated V-plot maps of $\log_2$ (Mot1 IP/input) data for the 2.5-min and 10-min MNase time points centered on the TATAWAWR motifs within the 438 peaks determined above. Nucleosomes were highly depleted from both IP samples (Fig. 3B), indicating a lack of interaction between Mot1 and nucleosomes and arguing against a direct role for Mot1 in nucleosome remodeling (23). Consistent with our aggregate plot results, robust enrichment of Mot1 was detected both over the TATA box and the DNA upstream of the TATA box (Fig. 3B). As V-plots impart information about the length of protected fragments, we were also able to determine that the footprint of Mot1 immediately upstream of TATA boxes is quite large, comprising fragments ~40 to 150 bp in length. The large size of this footprint likely reflects the interaction of Mot1 with the transcription machinery and may also indicate interaction of Mot1 with the SAGA (Spt-Ada-Gcn5-acetyltransferase) coactivator complex, which has been shown to promote TBP turnover (40). These results strongly suggest that the model of Mot1 action *in vitro*, where it associates with DNA upstream of TBP and then recognizes TBP from the upstream direction, reflects its function *in vivo*.

Loss of Mot1 function redistributes TBP from TATA-less to TATA-containing sites. The initial characterization of Mot1 as a TBP-displacing factor (6) suggested that loss of Mot1 would result in a global increase of TBP binding across the genome. However, it has been shown that loss of Mot1 function or loss of its interaction with TBP decreases TBP association with a number of sites in the genome (11, 12, 18, 19, 21), and the basis of this phenomenon has been unclear. To comprehensively address the effects of Mot1 loss on TBP binding to chromatin, we performed TBP ORGANIC profiling in strains harboring either the wild-type *MOT1* gene or

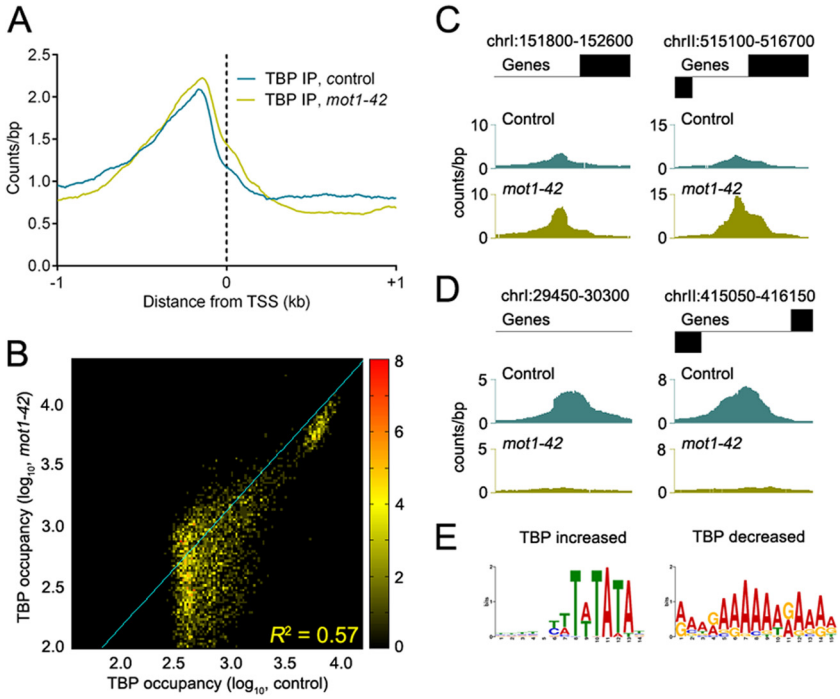

FIG 4 Inactivation of Mot1 causes redistribution of TBP from TATA-less to TATA-containing sites. (A) Aggregate plot of TBP control and *mot1-42* ORGANIC signal (10′ MNase) around TSSs. (B) Two-dimensional histogram comparing TBP occupancy levels at TBP peaks in the *mot1-42* strain with and without heat shock. (C) Two examples of TBP peaks that display increased TBP occupancy upon Mot1 inactivation. (D) Two examples of TBP peaks that display decreased TBP occupancy upon Mot1 inactivation. (E) Sequence logos of the highest scoring MEME-derived motif in the top 500 TBP peaks with increased TBP (left) and the top 500 peaks with decreased TBP (right) upon Mot1 inactivation.

the temperature-sensitive *mot1-42* allele. The protein produced from the *mot1-42* allele contains a single amino acid change (L383P) that renders it biochemically inactive at 35°C *in vitro* due to deficient TBP recognition (41). Consistent with previous work (16), inactivation of Mot1 led to a slight but significant ($P < 0.001$ by Kolmogorov-Smirnov test) overall increase in TBP occupancy at promoters (Fig. 4A), as well as a broadening of TBP signal downstream of the TSS.

We then assessed the effects of Mot1 inactivation on TBP occupancy at TBP peaks. Attenuation of the Mot1-TBP interaction by shifting to the restrictive temperature resulted in both increases and decreases in TBP occupancy at hundreds of TBP peak locations (Fig. 4B to D). Surprisingly, more TBP peaks lost than gained TBP upon inactivation of Mot1. Of the 3,002 TBP 10-min MNase peaks, 224 displayed a >2-fold increase in TBP binding following inactivation of Mot1, while 752 displayed a >2-fold decrease in TBP occupancy after temperature shift ($P = 4.43 \times 10^{-64}$ by chi-square analysis) (see Data Set S3 in the supplemental material). We obtained similar results with the 2.5-min MNase data set: of the 3,272 2.5-min MNase TBP peaks, 145 displayed a >2-fold increase in TBP binding following inactivation of Mot1, while 727 displayed a >2-fold decrease in TBP occupancy after temperature shift ($P = 1.81 \times 10^{-86}$ by chi-square analysis; Data Set S3). We noted that occupancies of TBP peaks mainly associated with tRNA genes (Fig. 4B, top right corner of the density plot) were largely unaffected by Mot1 inactivation, consistent with the insensitivity of Pol III promoters bound by the basal initiation factor transcription factor IIIB (TFIIIB) to Mot1 regulation (3).

It has been proposed that loss of Mot1 causes redistribution of TBP from intrinsically unfavorable to intrinsically favorable binding sites (18, 22). However, it is unclear what sequence features might define a favorable versus unfavorable site for TBP binding *in vivo*. We therefore used MEME-ChIP (31) to search the 500 sites with the highest level of TBP gain and loss after Mot1 inactivation for sequence motifs. Of the sites of TBP gain, 410/500 (82%) contained a robust TATA box ($E = 6.7 \times 10^{-196}$) (Fig. 4E). In striking contrast, no significant TATA box motif was detected in the class of sites that lost TBP; rather, 112/500 (22.4%) contained poly(dA-dT) tracts ($E = 2.0 \times 10^{-101}$) (Fig. 4E). We also scored the same sets of peaks using the TATA position weight matrix (PWM) derived from MEME (Table 2) and found that the sites that gained TBP in the *mot1-42* strain had significantly higher PWM scores ($P = 2.58 \times 10^{-170}$ by *t* test). We also scored peaks using two previously described TATA motif PWMs (42, 43) obtained from ScerTF (44) and again found that TBP-increased peaks were much more likely to contain a high-scoring TATA motif (Pachkov motif, $P = 1.34 \times 10^{-157}$; Zhu motif, $P = 1.72 \times 10^{-153}$ by *t* test). We conclude that inactivation of Mot1 results in a redistribution of TBP from TATA-less to TATA-containing sites.

TBP redistribution is associated with changes in gene expression. Presumably, loss of TBP at TATA-less promoters would result in decreased expression of the associated genes, while gain of TBP at TATA-containing promoters would increase gene expression. Indeed, it has been shown that AA-mediated depletion of Mot1 tends to reduce the expression of TATA-less genes (17). To ascertain the biological significance of changes in TBP binding that occur when Mot1 is inactivated, we plotted the change in TBP

TABLE 2 TBP PWM derived from the top 500 sites of TBP gain in *mot1-42*

Base position within motif	Probability of occurrence of:			
	A	C	G	T
1	0.180488	0.260976	0.14878	0.409756
2	0.14878	0.265854	0.180488	0.404878
3	0.185366	0.214634	0.156098	0.443902
4	0.153659	0.258537	0.143902	0.443902
5	0.182927	0.302439	0.231707	0.282927
6	0.056098	0.407317	0.065854	0.470732
7	0.292683	0.1	0.002439	0.604878
8	0	0.012195	0	0.987805
9	0.539024	0	0	0.460976
10	0.012195	0	0	0.987805
11	1	0	0	0
12	0.070732	0	0	0.929268
13	0.926829	0	0	0.073171
14	0.156098	0.202439	0.163415	0.478049

occupancy at promoters as a heat map ranked by the expression of the associated gene in the *mot1-42* mutant strain versus control (16). We found that genes with increased expression in *mot1-42* also displayed markedly increased TBP binding, while genes whose expression decreases in the *mot1-42* mutant strain were more likely to show reduced TBP binding (Fig. 5), indicating that the redistribution of TBP when Mot1 is inactivated has functional effects on gene expression.

DISCUSSION

Mot1, a relative of diverse ATP-dependent chromatin remodelers, plays a critical role in eukaryotic transcription through its regulation of TBP-genome association. We find that loss of Mot1 function causes TBP gain at sites containing TATA boxes but leads to loss of TBP binding at TATA-less sites. The redistribution of TBP in the absence of Mot1 function appears to have functional consequences: increased TBP binding is associated with increased gene expression, while decreased TBP binding is linked to decreased gene expression. These observations are consistent with a redistribution model, wherein Mot1 clears TBP from sites of intrinsic preference (TATA-containing sites) to ensure that there is sufficient soluble TBP to bind intrinsically disfavored (TATA-less) sites.

While the poly(dA-dT) runs found within peaks that lose TBP are most likely less favorable than a TATA box for TBP binding in terms of sequence preference, an additional property of poly(dA-dT) tracts may favor TBP binding. Poly(dA-dT) tracts cause narrowing of the minor groove and increase DNA stiffness, disfavoring nucleosome formation (45). Such exclusion of nucleosomes by poly(dA-dT) tracts would help to maintain DNA accessible to DNA-binding proteins, while serving as low-affinity binding sites for TBP liberated from TATA-containing sites by Mot1.

Our results bear on the action of Mot1 at TATA-containing versus TATA-less sites, particularly in the context of a model for Mot1 action *in vivo* proposed by Tora and Timmers (46). In this model, the sharp bending of TATA-containing DNA by TBP generates a "spring" for rapid Mot1-catalyzed TBP removal, leading to the previously described rapid turnover of TBP at these sites (40). This predicts that loss of Mot1 would result in increased TBP binding at these sites; indeed, we observed that 82% of the top 500 sites of TBP gain in the *mot1-42* strain contained robust TATA boxes. This model also suggests that Mot1 removes TBP from TATA-less promoters, albeit at a lower rate. This feature of the model would predict that, in the absence of Mot1 function, TATA-less promoters would also gain TBP. However, we found that this is not the case: TATA-less Pol II sites tended to lose TBP in the *mot1-42* strain. Interestingly, it has been suggested that TBP bound to TATA-less promoters may be inaccessible to Mot1 (18, 40). The differential sensitivity of TATA-containing versus TATA-less promoters may be attributable to their regulation by different coactivator complexes. The SAGA complex loads TBP onto TATA-containing promoters (47) and is also associated with high TBP turnover (40), suggesting that it synergizes with Mot1 in TBP removal, a hypothesis supported by the finding of negative genetic interaction between Mot1 and SAGA (17). In contrast, TATA-less promoters tend to be regulated by the TFIID coactivator complex (47). The human ortholog of Mot1, BTAF1, does not associate with TFIID (48) and is unable to inhibit transcription from TATA-less promoters bound by TFIID *in vitro* (3). TATA-less genes also tend to display low Mot1-dependent TBP turnover *in vivo* (40). Last, sequential ChIP experiments have suggested mutually exclusive association of Mot1 and TFIID at a few promoters (49). The recently solved structure of the TFIID component TAF1 (TATA box-binding protein-associated factor 1) in complex with TBP suggests a mechanism by which TFIID might render TBP refractory to removal from DNA by Mot1 (50). TAF1 contacts the same surfaces of TBP as Mot1 does, and it therefore stands to reason that, by interacting with TAF1, TBP in the context of TFIID is shielded from interaction with and dissociation by Mot1. *In vivo* support for this structural model derives from the observation that TAF1 is highly enriched at TATA-less promoters but depleted from TATA-containing promoters in yeast (29). Furthermore, depletion of yeast TAF1 results in increased TBP mobility (51), and TAF1 depletion in *Drosophila* cells leads to dissociation of TBP from TFIID (52, 53) as well as increases in nascent RNA production from TATA-containing promoters (52). As

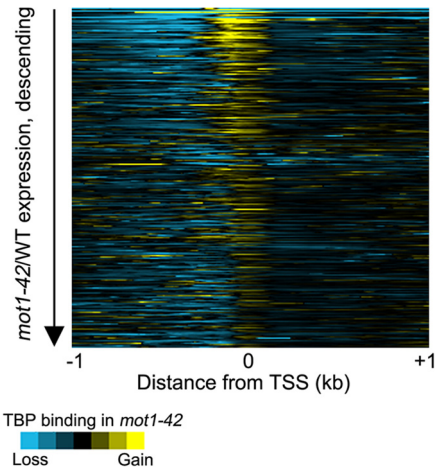

FIG 5 Loss of Mot1 results in correlated changes in gene expression and TBP binding. Heat map of the change in TBP binding between the *mot1-42* strain and control (wild type [WT]) strain (10′ MNase) around TSSs. The heat map is shown in descending order by the change in expression of the associated gene in the *mot1-42* strain.

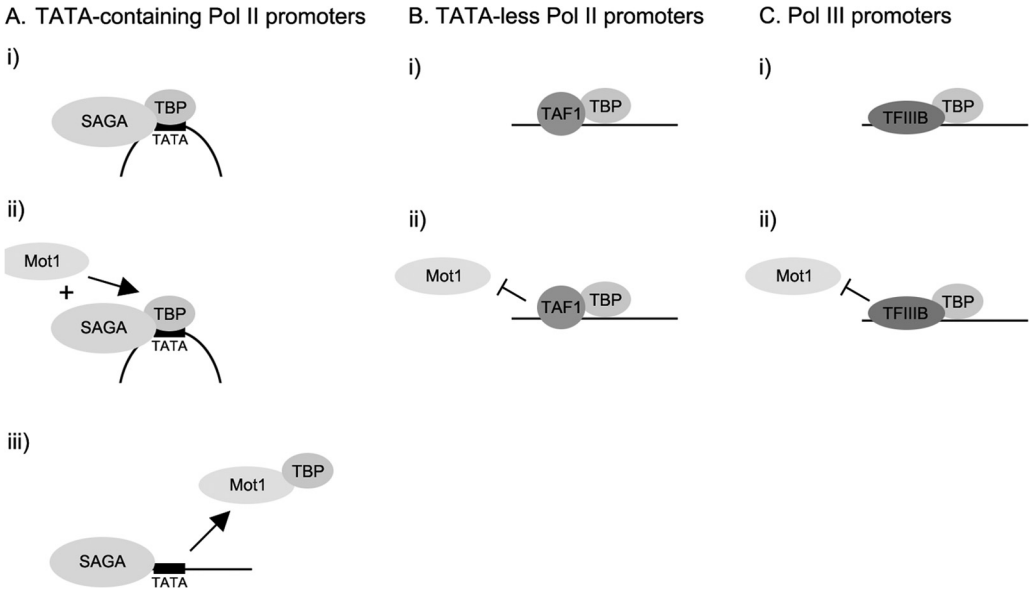

FIG 6 A model for the relationship of Mot1 and TBP at various classes of promoters. (A) The relationship between Mot1 and TBP at TATA-containing Pol II promoters. (i) TBP binds and sharply bends TATA DNA in the context of the SAGA complex. (ii) Mot1 associates with the TBP-DNA complex and synergizes with SAGA to rapidly dissociate TBP from DNA (iii). (B) The relationship between Mot1 and TBP at TATA-less Pol II promoters. (i) TBP binds DNA in the context of the TFIID complex (for clarity, only TAF1 is shown). (ii) The interaction of TBP with TAF1 impairs recognition of TBP by Mot1, leading to continued TBP binding. (C) The relationship between Mot1 and TBP at Pol III promoters. (i) TBP binds DNA as part of TFIIIB. (ii) The interaction of TBP with an unspecified component(s) of TFIIIB impairs the Mot1-TBP interaction, leading to sustained TBP binding.

TATA-less promoters are likely to be lower-affinity sites for TBP binding, the protection of TBP from Mot1-mediated dissociation by TAF1 may serve to ensure that sufficient TBP remains associated with these promoters for appropriate transcriptional activation. An analogous situation might occur at Pol III promoters, which tend to be TATA-less and insensitive to TBP displacement by Mot1 (3). Protection of TBP from Mot1 displacement at Pol III promoters may be achieved by the interaction of TBP with a component(s) of the TFIIIB complex.

We propose that the primary site of the TBP-displacing activity of Mot1 *in vivo* is at TATA boxes and that Mot1 may not function to displace TBP from TATA-less promoters. TATA boxes likely represent intrinsically preferred sites of TBP binding that also facilitate TBP displacement by Mot1 via the generation of the bent DNA "spring" as well as cooperation with the SAGA complex (Fig. 6A). At TATA-less sites, regulated by TFIID, Mot1 is unable to interact with TBP due to the interaction of TAF1 with the Mot1-interacting surface of TBP, resulting in continued binding of TBP (Fig. 6B). We propose a similar situation for Pol III promoters, wherein a component of TFIIIB interacts with the Mot1-interacting surface of TBP, inhibiting its interaction with Mot1 and ensuring persistence of TBP association (Fig. 6C). Mechanistically, our data indicate that the displacement of TBP from TATA boxes by Mot1 maintains sufficient soluble TBP such that TATA-less sites can also be bound. Loss of Mot1 thus results in increased TBP binding to its intrinsically preferred (TATA-containing) binding sites, depleting the soluble pool of TBP and reducing TBP association with intrinsically disfavored (TATA-less) sites.

ACKNOWLEDGMENTS

We thank Jorja Henikoff for assistance with data analysis, Siva Kasinathan for comments on the manuscript, and David Auble for helpful discussions and yeast strains.

This work was supported by NIH grants 5U01 HG004274, U54 CA143862, R01 ES020116, and 5T32 CA009657 (FHCRC Chromosome Metabolism and Cancer Training Grant) and by the Howard Hughes Medical Institute.

REFERENCES

1. **Hernandez N.** 1993. TBP, a universal eukaryotic transcription factor? Genes Dev. **7:**1291–1308.
2. **Huisinga K, Pugh BF.** 2007. A TATA binding protein regulatory network that governs transcription complex assembly. Genome Biol. **8:**R46. doi:10.1186/gb-2007-8-4-r46.
3. **Chicca JJ, Auble DT, Pugh BF.** 1998. Cloning and biochemical characterization of TAF-172, a human homolog of yeast Mot1. Mol. Cell. Biol. **18:**1701–1710.
4. **Davis JL, Kunisawa R, Thorner J.** 1992. A presumptive helicase (MOT1 gene product) affects gene expression and is required for viability in the yeast Saccharomyces cerevisiae. Mol. Cell. Biol. **12:**1879–1892.
5. **Wansleeben C, van Gurp L, de Graaf P, Mousson F, Timmers HTM, Meijlink F.** 2011. An ENU-induced point mutation in the mouse Btaf1 gene causes post-gastrulation embryonic lethality and protein instability. Mech. Dev. **128:**279–288.
6. **Auble DT, Hansen KE, Mueller CG, Lane WS, Thorner J, Hahn S.** 1994. Mot1, a global repressor of RNA polymerase II transcription, inhibits TBP binding to DNA by an ATP-dependent mechanism. Genes Dev. **8:**1920–1934.
7. **Darst RP, Wang D, Auble DT.** 2001. MOT1-catalyzed TBP-DNA disruption: uncoupling DNA conformational change and role of upstream DNA. EMBO J. **20:**2028–2040.
8. **Moyle-Heyrman G, Viswanathan R, Widom J, Auble DT.** 2012. Two-step mechanism for modifier of transcription 1 (Mot1) enzyme-catalyzed displacement of TATA-binding protein (TBP) from DNA. J. Biol. Chem. **287:**9002–9012.
9. **Sprouse RO, Brenowitz M, Auble DT.** 2006. Snf2/Swi2-related ATPase Mot1 drives displacement of TATA-binding protein by gripping DNA. EMBO J. **25:**1492–1504.
10. **Wollmann P, Cui S, Viswanathan R, Berninghausen O, Wells MN, Moldt M, Witte G, Butryn A, Wendler P, Beckmann R, Auble DT, Hopfner K-P.** 2011. Structure and mechanism of the Swi2/Snf2 remodeller Mot1 in complex with its substrate TBP. Nature **475:**403–407.

11. **Andrau J-C, Van Oevelen CJC, Van Teeffelen HAAM, Weil PA, Holstege FCP, Timmers HTM.** 2002. Mot1p is essential for TBP recruitment to selected promoters during in vivo gene activation. EMBO J. **21:**5173–5183.
12. **Choukrallah M-A, Kobi D, Martianov I, Pijnappel WWMP, Mischerikow N, Ye T, Heck AJR, Timmers HTM, Davidson I.** 2012. Interconversion between active and inactive TATA-binding protein transcription complexes in the mouse genome. Nucleic Acids Res. **40:**1446–1459.
13. **Dasgupta A, Darst RP, Martin KJ, Afshari CA, Auble DT.** 2002. Mot1 activates and represses transcription by direct, ATPase-dependent mechanisms. Proc. Natl. Acad. Sci. U. S. A. **99:**2666–2671.
14. **Hsu J-Y, Juven-Gershon T, Marr MT, Wright KJ, Tjian R, Kadonaga JT.** 2008. TBP, Mot1, and NC2 establish a regulatory circuit that controls DPE-dependent versus TATA-dependent transcription. Genes Dev. **22:**2353–2358.
15. **Madison JM, Winston F.** 1997. Evidence that Spt3 functionally interacts with Mot1, TFIIA, and TATA-binding protein to confer promoter-specific transcriptional control in Saccharomyces cerevisiae. Mol. Cell. Biol. **17:**287–295.
16. **Poorey K, Sprouse RO, Wells MN, Viswanathan R, Bekiranov S, Auble DT.** 2010. RNA synthesis precision is regulated by preinitiation complex turnover. Genome Res. **20:**1679–1688.
17. **Spedale G, Meddens CA, Koster MJE, Ko CW, van Hooff SR, Holstege FCP, Timmers HTM, Pijnappel WWMP.** 2012. Tight cooperation between Mot1p and NC2β in regulating genome-wide transcription, repression of transcription following heat shock induction and genetic interaction with SAGA. Nucleic Acids Res. **40:**996–1008.
18. **Venters BJ, Irvin JD, Gramlich P, Pugh BF.** 2011. Genome-wide transcriptional dependence on conserved regions of Mot1. Mol. Cell. Biol. **31:**2253–2261.
19. **Biswas D, Yu Y, Mitra D, Stillman DJ.** 2006. Genetic interactions between Nhp6 and Gcn5 with Mot1 and the Ccr4–Not complex that regulate binding of TATA-binding protein in Saccharomyces cerevisiae. Genetics **172:**837–849.
20. **Dasgupta A, Juedes SA, Sprouse RO, Auble DT.** 2005. Mot1-mediated control of transcription complex assembly and activity. EMBO J. **24:**1717–1729.
21. **van Oevelen CJC, van Teeffelen HAAM, Timmers HTM.** 2005. Differential requirement of SAGA subunits for Mot1p and Taf1p recruitment in gene activation. Mol. Cell. Biol. **25:**4863–4872.
22. **Auble DT.** 2009. The dynamic personality of TATA-binding protein. Trends Biochem. Sci. **34:**49–52.
23. **Topalidou I, Papamichos-Chronakis M, Thireos G, Tzamarias D.** 2004. Spt3 and Mot1 cooperate in nucleosome remodeling independently of TBP recruitment. EMBO J. **23:**1943–1948.
24. **Haruki H, Nishikawa J, Laemmli UK.** 2008. The anchor-away technique: rapid, conditional establishment of yeast mutant phenotypes. Mol. Cell **31:**925–932.
25. **Gelbart ME, Rechsteiner T, Richmond TJ, Tsukiyama T.** 2001. Interactions of Isw2 chromatin remodeling complex with nucleosomal arrays: analyses using recombinant yeast histones and immobilized templates. Mol. Cell. Biol. **21:**2098–2106.
26. **Zentner GE, Tsukiyama T, Henikoff S.** 2013. ISWI and CHD chromatin remodelers bind promoters but act in gene bodies. PLoS Genet. **9:**e1003317. doi:10.1371/journal.pgen.1003317.
27. **Henikoff JG, Belsky JA, Krassovsky K, MacAlpine DM, Henikoff S.** 2011. Epigenome characterization at single base-pair resolution. Proc. Natl. Acad. Sci. U. S. A. **108:**18318–18323.
28. **Zentner GE, Saiakhova A, Manaenkov P, Adams MD, Scacheri PC.** 2011. Integrative genomic analysis of human ribosomal DNA. Nucleic Acids Res. **39:**4949–4960.
29. **Rhee HS, Pugh BF.** 2012. Genome-wide structure and organization of eukaryotic pre-initiation complexes. Nature **483:**295–301.
30. **Harismendy O, Gendrel C-G, Soularue P, Gidrol X, Sentenac A, Werner M, Lefebvre O.** 2003. Genome-wide location of yeast RNA polymerase III transcription machinery. EMBO J. **22:**4738–4747.
31. **Machanick P, Bailey TL.** 2011. MEME-ChIP: motif analysis of large DNA datasets. Bioinformatics **27:**1696–1697.
32. **Grant CE, Bailey TL, Noble WS.** 2011. FIMO: scanning for occurrences of a given motif. Bioinformatics **27:**1017–1018.
33. **van Werven FJ, van Bakel H, van Teeffelen HAAM, Altelaar AFM, Koerkamp MG, Heck AJR, Holstege FCP, Timmers HTM.** 2008. Cooperative action of NC2 and Mot1p to regulate TATA-binding protein function across the genome. Genes Dev. **22:**2359–2369.
34. **Venters BJ, Wachi S, Mavrich TN, Andersen BE, Jena P, Sinnamon AJ, Jain P, Rolleri NS, Jiang C, Hemeryck-Walsh C, Pugh BF.** 2011. A comprehensive genomic binding map of gene and chromatin regulatory proteins in Saccharomyces. Mol. Cell **41:**480–492.
35. **Zanton SJ, Pugh BF.** 2004. Changes in genomewide occupancy of core transcriptional regulators during heat stress. Proc. Natl. Acad. Sci. U. S. A. **101:**16843–16848.
36. **Geisberg JV, Moqtaderi Z, Kuras L, Struhl K.** 2002. Mot1 associates with transcriptionally active promoters and inhibits association of NC2 in Saccharomyces cerevisiae. Mol. Cell. Biol. **22:**8122–8134.
37. **Kuras L, Struhl K.** 1999. Binding of TBP to promoters in vivo is stimulated by activators and requires Pol II holoenzyme. Nature **399:**609–613.
38. **Zentner GE, Henikoff S.** 2012. Surveying the epigenomic landscape, one base at a time. Genome Biol. **13:**250. doi:10.1186/gb4051.
39. **Sprouse RO, Shcherbakova I, Cheng H, Jamison E, Brenowitz M, Auble DT.** 2008. Function and structural organization of Mot1 bound to a natural target promoter. J. Biol. Chem. **283:**24935–24948.
40. **van Werven FJ, van Teeffelen HAAM, Holstege FCP, Timmers HTM.** 2009. Distinct promoter dynamics of the basal transcription factor TBP across the yeast genome. Nat. Struct. Mol. Biol. **16:**1043–1048.
41. **Darst RP, Dasgupta A, Zhu C, Hsu J-Y, Vroom A, Muldrow T, Auble DT.** 2003. Mot1 regulates the DNA binding activity of free TATA-binding protein in an ATP-dependent manner. J. Biol. Chem. **278:**13216–13226.
42. **Pachkov M, Erb I, Molina N, van Nimwegen E.** 2007. SwissRegulon: a database of genome-wide annotations of regulatory sites. Nucleic Acids Res. **35:**D127–D131.
43. **Zhu C, Byers KJRP, McCord RP, Shi Z, Berger MF, Newburger DE, Saulrieta K, Smith Z, Shah MV, Radhakrishnan M, Philippakis AA, Hu Y, De Masi F, Pacek M, Rolfs A, Murthy T, LaBaer J, Bulyk ML.** 2009. High-resolution DNA-binding specificity analysis of yeast transcription factors. Genome Res. **19:**556–566.
44. **Spivak AT, Stormo GD.** 2012. ScerTF: a comprehensive database of benchmarked position weight matrices for Saccharomyces species. Nucleic Acids Res. **40:**D162–D168.
45. **Segal E, Widom J.** 2009. Poly(dA:dT) tracts: major determinants of nucleosome organization. Curr. Opin. Struct. Biol. **19:**65–71.
46. **Tora L, Timmers HTM.** 2010. The TATA box regulates TATA-binding protein (TBP) dynamics in vivo. Trends Biochem. Sci. **35:**309–314.
47. **Basehoar AD, Zanton SJ, Pugh BF.** 2004. Identification and distinct regulation of yeast TATA box-containing genes. Cell **116:**699–709.
48. **Poon D, Campbell AM, Bai Y, Weil PA.** 1994. Yeast Taf170 is encoded by MOT1 and exists in a TATA box-binding protein (TBP)-TBP-associated factor complex distinct from transcription factor IID. J. Biol. Chem. **269:**23135–23140.
49. **Geisberg JV, Struhl K.** 2004. Cellular stress alters the transcriptional properties of promoter-bound Mot1-TBP complexes. Mol. Cell **14:**479–489.
50. **Anandapadamanaban M, Andresen C, Helander S, Ohyama Y, Siponen MI, Lundström P, Kokubo T, Ikura M, Moche M, Sunnerhagen M.** 2013. High-resolution structure of TBP with TAF1 reveals anchoring patterns in transcriptional regulation. Nat. Struct. Mol. Biol. **20:**1008–1014.
51. **Sprouse RO, Karpova TS, Mueller F, Dasgupta A, McNally JG, Auble DT.** 2008. Regulation of TATA-binding protein dynamics in living yeast cells. Proc. Natl. Acad. Sci. U. S. A. **105:**13304–13308.
52. **Pennington KL, Marr SK, Chirn G-W, Marr MT.** 2013. Holo-TFIID controls the magnitude of a transcription burst and fine-tuning of transcription. Proc. Natl. Acad. Sci. U. S. A. **110:**7678–7683.
53. **Wright KJ, Marr MT, Tjian R.** 2006. TAF4 nucleates a core subcomplex of TFIID and mediates activated transcription from a TATA-less promoter. Proc. Natl. Acad. Sci. U. S. A. **103:**12347–12352.